

---

# JOURNAL OF THE AMERICAN CHEMICAL SOCIETY

---

## Computational Study of Tunneling and Coupled Motion in Alcohol Dehydrogenase-Catalyzed Reactions: Implication for Measured Hydrogen and Carbon Isotope Effects

Joseph Rucker<sup>†</sup> and Judith P. Klinman\*

Contribution from the Department of Chemistry, University of California, Berkeley, California 94720

Received July 9, 1998

**Abstract:** The relationship between the two hydrogen isotope effects,  $k_H/k_T$  and  $k_D/k_T$ , can provide a probe for the role of tunneling and coupled motion in enzyme-catalyzed reactions.<sup>1,2</sup> Using vibrational analysis and the Bigeleisen–Mayer equation, we have developed a simple computational model to explain the unusual exponential relationships that have been experimentally observed in the yeast alcohol dehydrogenase (YADH)<sup>3</sup>-catalyzed oxidation of benzyl alcohol.<sup>2</sup> The experimental results are fitted by a model that has both substantial hydrogen tunneling and coupling between the reaction coordinate and a large number of vibrational modes. We show that the secondary  $k_D/k_T$  isotope effect is expected to be the most sensitive parameter to changes in reaction coordinate properties. A high degree of coupled motion leads to an unexpected suppression of the semiclassical secondary isotope effects, resulting in secondary isotope effects which are primarily manifestations of tunneling. This has implications for the use of secondary hydrogen isotope effects as probes of transition state position. During the course of these computational studies, primary carbon isotope effects were shown to undergo a consistent increase in magnitude upon substitution of the transferring protium with deuterium. We suggest that this effect can be explained using simple semiclassical principles and will apply to a broad range of reactions. Inference of reaction mechanism from the observation of a change in a heavy-atom isotope effects upon substrate deuteration should be interpreted with caution when the position of heavy atom and hydrogen isotope substitution are the same.

### Introduction

Kinetic isotope effects are versatile probes of transition state structure and are widely used by physical organic chemists and enzymologists to understand reaction mechanisms.<sup>4</sup> The interpretation of kinetic isotope effects most often used by research-

<sup>†</sup> Present address: Department of Pathology and Laboratory Medicine, University of Pennsylvania, Philadelphia, PA 19103.

\* To whom correspondence should be addressed. J.P.K. is also in the Department of Molecular and Cell Biology, University of California, Berkeley.

(1) Saunders, W. H., Jr. *J. Am. Chem. Soc.* **1985**, *107*, 164–169.

(2) Cha, Y.; Murray, C. J.; Klinman, J. P. *Science* **1989**, *243*, 1325–1330.

(3) The following abbreviations have been used: YADH, yeast alcohol dehydrogenase; HLADH, horse liver alcohol dehydrogenase; FDH, formate dehydrogenase; G<sub>6</sub>PDH, glucose 6-phosphate dehydrogenase; ALDH, yeast aldehyde dehydrogenase.

ers derives from the theoretical description of isotope effects originally presented by Bigeleisen and Mayer.<sup>5,6</sup> This theory, based on an application of equilibrium statistical mechanics to transition state theory, is called a semiclassical model: stable vibrations, both in the ground state and in the transition state, are treated quantum mechanically while the reaction coordinate, describing the motion of the transferred hydrogen, is treated classically.

It has long been realized that quantum-mechanical tunneling can contribute to hydrogen transfer.<sup>6–9</sup> A variety of approaches

(4) Melander, L.; Saunders, W. H., Jr. *Reaction Rates of Isotopic Molecules*; Robert I. Krieger Publ. Co.: Malabar, FL, 1987.

(5) Bigeleisen, J.; Goepert-Mayer, M. *J. Chem. Phys.* **1947**, *15*, 261–267.

(6) Bigeleisen, J. *J. Chem. Phys.* **1949**, *17*, 675–678.

(7) Caldin, E. F. *Chem. Rev.* **1969**, *69*, 135–156.

have been developed to probe the role of tunneling in hydrogen transfer reactions, particularly with respect to hydrogen isotope effects. The most commonly used isotopic approach is the temperature dependence of isotope effects, where tunneling is expected to lead to deviations from the semiclassical (Arrhenius) behavior of isotope effects.<sup>7</sup> Such effects have been seen in a number of solution and enzymatic reactions and have been analyzed by a variety of theoretical approaches.<sup>1,7,10–16</sup>

Another isotopic probe of tunneling is the use of exponential relationships between isotope effects (at both primary and secondary hydrogen positions).<sup>17</sup> In practice, exponential relationships have proven more difficult to detect and to interpret. Of these, the most commonly used is the Swain–Schaad relationship (also referred to as relative isotope effects):<sup>18</sup>

$$\left(\frac{k_{\text{H}}}{k_{\text{T}}}\right) = \left(\frac{k_{\text{D}}}{k_{\text{T}}}\right)^s \quad (1)$$

where  $s$  is expected to be within the range 3.26–3.34 under semiclassical conditions, with some authors suggesting a somewhat wider range.<sup>19,20</sup> Positive deviations from this range are considered to be an indication of tunneling, although the expected magnitudes of such deviations have been difficult to quantify.<sup>1,21–23</sup> It should be noted that the Swain–Schaad relationship is more often written as relating  $k_{\text{H}}/k_{\text{D}}$  to  $k_{\text{H}}/k_{\text{T}}$ .

Another exponential relationship is the rule of the geometric mean (RGM), which states that there are no isotope effects on isotope effects:

$$\left(\frac{k_{\text{L}}}{k_{\text{T}}}\right)_{\text{H}} = \left(\frac{k_{\text{L}}}{k_{\text{T}}}\right)_{\text{D}} \quad (2)$$

where L is either H or D and  $r$  is the RGM exponent.<sup>24</sup> The subscript H or D describes isotopic substitution in an unmeasured position. In the case of simple semiclassical isotope effects,  $r$  is approximately equal to 1 and there is no effect of remote deuteration on either a ( $k_{\text{H}}/k_{\text{T}}$ ) or ( $k_{\text{D}}/k_{\text{T}}$ ) isotope effect.<sup>24</sup> Deviations from the RGM can arise from both semiclassical

and tunneling considerations.<sup>1,25,26</sup> Studies of isotopic disproportionation equilibria (such as  $\text{H}_2\text{O}/\text{D}_2\text{O}$ ) demonstrate the existence of measurable semiclassical RGM deviations.<sup>25,27</sup> Semiclassical deviations from RGM behavior in kinetic systems, as defined by eq 2, have been more difficult to understand.<sup>28–31</sup> Saunders has published calculations of both semiclassical and full (semiclassical plus tunneling) isotope effects for a series of elimination reactions.<sup>1</sup> Although he did not analyze semiclassical RGM deviations explicitly, some  $r$  values can be derived from the published results. In general, semiclassical hydrogen isotope effects demonstrated  $r$  values that were less than unity. The inclusion of tunneling in such systems, however, produced RGM deviations with  $r$  greater than unity, consistent with published experiments. Sizable positive deviations from the RGM appear to require, in general, a coupling of motion between two hydrogenic sites, e.g., a reaction where a hydrogen atom is transferred concomitant with the reorganizational motion of a second hydrogenic site, together with the occurrence of hydrogen tunneling.<sup>1,26,32</sup> It should be noted that RGM deviations are most commonly described in the literature as the ratio between two isotope effects of interest or as the inequality between a double-isotopic substitution and the product of its two corresponding single-isotope substitutions.

In a mixed-label experiment, both sites of isotopic substitution are altered:

$$\left(\frac{k_{\text{H}}}{k_{\text{T}}}\right)_{\text{H}} = \left(\frac{k_{\text{D}}}{k_{\text{T}}}\right)_{\text{D}}^y \quad (3)$$

The exponent,  $y$ , is the product of a Swain–Schaad exponent,  $s$ , and a rule of the geometric mean exponent,  $r$ .<sup>32</sup> Thus, a value of  $y$  greater than 3.3 should be indicative of tunneling. The exponent,  $y$ , is probably the most sensitive probe of tunneling since both Swain–Schaad and RGM deviations will contribute to observed deviations in systems with tunneling plus coupled motion.

Positive deviations of  $y$  have been seen in the mixed-label experiments performed by Cha.<sup>2</sup> In these experiments, Cha measured isotope effects on the YADH-catalyzed oxidation of benzyl alcohol by  $\text{NAD}^+$ : Focusing on the primary and secondary hydrogens of benzyl alcohol, Cha measured  $y$  values of 3.58 and 10.2 for primary and secondary isotope effects, respectively. Such values for  $y$  are clear indications of the presence of tunneling and coupled motion. Deviations of this nature have also been seen in a number of other enzymatic and chemical systems.<sup>13,33–35</sup>

Though deviations from semiclassical exponential relationships have been experimentally measured, the conditions under

(8) Bell, R. P. *The Tunnel Effect in Chemistry*; Chapman and Hall: London, 1980.

(9) Sühnel, J.; Schowen, R. L. Theoretical Basis for Primary and Secondary Hydrogen Isotope Effects. In *Enzyme Mechanism from Isotope Effects*; Cook, P. F., Ed; CRC Press: Boca Raton, FL, 1991; pp 3–35.

(10) Schneider, M. E.; Stern, M. J. *J. Am. Chem. Soc.* **1972**, *94*, 1517–1522.

(11) Stern, M. J.; Weston, R. E., Jr. *J. Chem. Phys.* **1974**, *60*, 2808–2814.

(12) Kim, Y.; Kreevoy, M. M. *J. Am. Chem. Soc.* **1992**, *114*, 7116–7123.

(13) Lin, S.; Saunders, W. H., Jr. *J. Am. Chem. Soc.* **1994**, *116*, 6107–6110.

(14) Amin, M.; Saunders, W. H., Jr. *J. Phys. Org. Chem.* **1993**, *6*, 393–398.

(15) Grant, K. L.; Klinman, J. P. *Biochemistry* **1989**, *28*, 6597–6605.

(16) Jonsson, T.; Edmonson, D. E.; Klinman, J. P. *Biochemistry* **1994**, *33*, 14871–14878.

(17) Klinman, J. P. Hydrogen Tunneling and Coupled Motion in Enzyme Reactions. In *Enzyme Mechanism from Isotope Effects*; Cook, P. F., Ed.; CRC Press: Boca Raton, FL, 1991; pp 127–148.

(18) Swain, C. G.; Stivers, E. C.; Reuwer, J. F., Jr.; Schaad, L. J. *J. Am. Chem. Soc.* **1958**, *107*, 5885–5893.

(19) Bigeleisen, J. Correlation of Tritium and Deuterium Isotope Effects. In *Tritium in the Physical and Biological Sciences*; International Atomic Energy Agency: Vienna, 1962; pp 161–168.

(20) Stern, M. J.; Vogel, P. C. *J. Am. Chem. Soc.* **1971**, *93*, 4664–4675.

(21) Lewis, E. S.; Robinson, J. K. *J. Am. Chem. Soc.* **1968**, *90*, 4337–4344.

(22) Stern, M. J.; Weston, R. E., Jr. *J. Chem. Phys.* **1974**, *60*, 2815–2821.

(23) Grant, K. L.; Klinman, J. P. *Bioorg. Chem.* **1992**, *20*, 1–8.

(24) Bigeleisen, J. *J. Chem. Phys.* **1955**, *23*, 2264–2267.

(25) Ishida, T.; Bigeleisen, J. *J. Chem. Phys.* **1976**, *64*, 4775–4789.

(26) Huskey, W. P.; Schowen, R. L. *J. Am. Chem. Soc.* **1983**, *105*, 5704–5706.

(27) Wolfsberg, M.; Massa, A. A.; Pyper, J. W. *J. Chem. Phys.* **1970**, *53*, 3138–3146.

(28) Ostovic, D.; Roberts, R. M. G.; Kreevoy, M. M. *J. Am. Chem. Soc.* **1983**, *105*, 7629–7631.

(29) Hermes, J. D.; Morrical, S. W.; O’Leary, M. H.; Cleland, W. W. *Biochemistry* **1984**, *23*, 5479–5488.

(30) Hermes, J. D.; Cleland, W. W. *J. Am. Chem. Soc.* **1984**, *106*, 7263–7264.

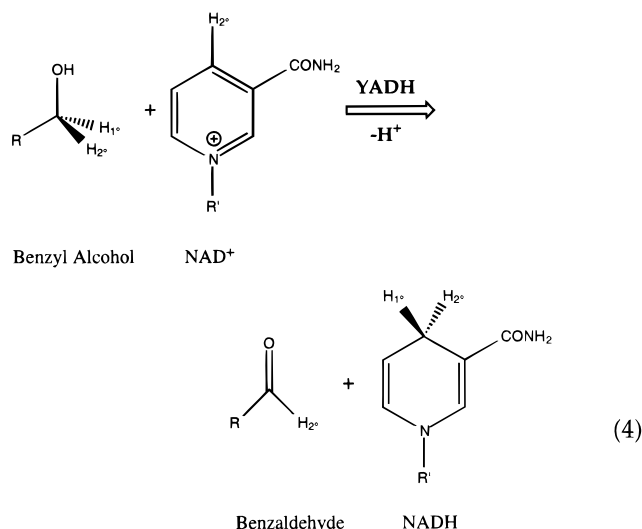
(31) Kurz, L. C.; Frieden, C. *J. Am. Chem. Soc.* **1980**, *102*, 4198–4203.

(32) Huskey, W. P. *Phys. Org. Chem.* **1991**, *4*, 361–366.

(33) Amin, M.; Price, R. C.; Saunders, W. H., Jr. *J. Am. Chem. Soc.* **1990**, *112*, 4467–4471.

(34) Bahnon, B. J.; Park, D.-H.; Kim, K.; Plapp, B. V.; Klinman, J. P. *Biochemistry* **1993**, *31*, 5503–5507.

(35) Alston, W. C.; Kanska, M.; Murray, C. J. *Biochemistry* **1996**, *35*, 12873–12881.



which such deviations will appear are difficult to predict. Some reactions which do not indicate unusual exponential behavior between  $k_D/k_T$  and  $k_H/k_T$  have been shown to exhibit tunneling behavior using other isotopic methods such as temperature dependence.<sup>15,16</sup> In an effort to explain this phenomenon, Grant and Klinman applied a truncated Bell correction to the calculation of primary isotope effects, finding that exponents typical of semiclassical reactions may be observed when both heavy and light isotopes are undergoing extensive tunneling.<sup>23</sup>

Huskey and Schowen,<sup>26</sup> focusing on solution and enzymatic  $\text{NAD}^+$ -dependent reactions, have discussed isotope effects in systems where primary and secondary hydrogenic motion are coupled in the transition state. These reactions are distinguished by having  $\alpha$ -secondary kinetic isotope effects which may be larger than the corresponding  $\alpha$ -secondary equilibrium isotope effects, a result which is inconsistent with the general view of secondary isotope effects being probes of transition state position. Huskey and Schowen demonstrated that such behavior is consistent with a model where there is coupled motion between primary and secondary hydrogens in the transition state reaction coordinate as well as moderate amounts of tunneling. Importantly, their model predicts that deviations from the RGM should be seen on both primary and  $\alpha$ -secondary isotope effects. RGM deviations were subsequently reported with formate dehydrogenase, where the  $\alpha$ -secondary  $\text{NAD}^+$  isotope effect was reduced from 1.23 to 1.07 upon primary deuteration.<sup>29</sup>

Drawing on this work, Saunders presented a computational study indicating that Swain–Schaad deviations between  $k_H/k_T$  and  $k_D/k_T$  could be used as a probe of tunneling.<sup>1</sup> The circumstances under which deviations are expected in both primary and secondary isotope effects include coupled motion, tunneling, and multiple isotopic labeling. The degree of apparent deviation from semiclassical behavior was, in fact, anticipated to be larger for secondary than primary isotope effects, as subsequently reported in the case of YADH.<sup>2</sup> This is a simple consequence of the smaller magnitude of secondary isotope effects and does not, in any way, imply greater tunneling at the secondary position. Huskey later pointed out that the measured deviations in the YADH case were, in fact, not pure Swain–Schaad deviations (eq 1) but rather mixed RGM/Swain–Schaad deviations (eq 3).<sup>32</sup> Using a hydride transfer modeling scheme, he showed that most of the observed deviations in  $y$  for secondary isotope effects could be explained as RGM deviations, emphasizing the importance of the particular isotopic labeling scheme used in the experiments.

This last study demonstrated that the unusual exponential deviations seen in both computational and experimental studies were consistent with a model employing coupled motion and tunneling. However, in none of the computational studies (or studies of solution reactions)<sup>13,33</sup> were deviations on the order of those seen in YADH observed.<sup>2</sup> We have used a modeling scheme similar to that used by Huskey and Schowen to reproduce the unusual isotope effects seen in YADH. The results show that the secondary  $k_D/k_T$  isotope effect is the most sensitive to reaction coordinate structure and further emphasizes that secondary isotope effects, in general, are not probes of transition state position at carbon centers undergoing hydrogen abstraction and extensive rehybridization. The isotope dependence of the reaction coordinate frequency is found to be a critical parameter for proper modeling of the experimental data. Our final model indicates that the reaction coordinate isotope dependence is sensitive to implicit heavy-atom motion as well as to explicit coupling between primary and secondary hydrogens.

In addition to being probes of transition state structure, enzymologists have also used isotope effects to elucidate kinetic complexity, i.e., the relationship of a hydrogen transfer step to other potential rate-limiting steps in the enzyme reaction mechanism.<sup>36</sup> Candidates for these latter steps include the dissociation of substrate/product, conformational changes, and other, nonisotopically sensitive chemical steps. A particularly elegant method, developed by Cleland and co-workers,<sup>30,36</sup> utilizes combinations of hydrogen and carbon (or other heavy-atom) isotope effects to determine the degree of rate limitation by a hydrogen transfer step. This method is based on the assumption that hydrogen and carbon isotope effects are independent of one another, i.e., that the rule of the geometric mean holds for the two isotope effects:

$$\left(\frac{k_{12\text{C}}}{k_{13\text{C}/\text{H}}}\right) = \left(\frac{k_{12\text{C}}}{k_{13\text{C}}}\right)_{\text{D}} \quad (5)$$

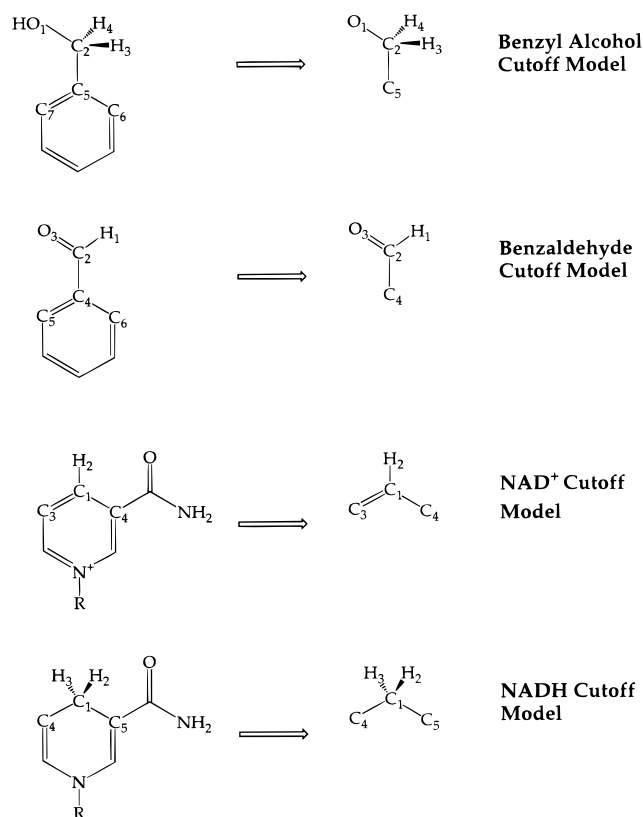
Making this assumption, changes in an observed carbon isotope effect with changes in hydrogen isotope are related to the degree to which the carbon isotope effect is fully expressed.

During our studies of isotope effects in YADH-catalyzed reactions, it appeared that our computational model was showing deviations from the carbon RGM when the carbon undergoing hydrogen transfer was labeled with both  $^{13}\text{C}$  and deuterium. Further analysis brought to light that these deviations were caused by both semiclassical and tunneling considerations. This result indicates that labeling of a single reacting center with two isotopes can give rise to patterns in measured isotope effects that may not be indicative of kinetic complexity.

## Methods

We used the Bigeleisen–Mayer equation to calculate isotope effects for the YADH-catalyzed oxidation of benzyl alcohol by  $\text{NAD}^+$  (eq 4).<sup>5,6,37</sup> This equation requires only knowledge of vibrational frequencies and their isotopic dependencies for reactants and transition states in order to calculate isotope effects. Since isotope effects are local phenomena, only the parts of the molecule containing the isotopically labeled atom(s) need be included. Wolfsberg and Stern have shown that one can generally remove atoms that are more than two bonds removed from the site of interest without changing the essential

(36) Cleland, W. W. Multiple Isotope Effects in Enzyme-Catalyzed Reactions. In *Enzyme Mechanism for Isotope Effects*; Cook, P. F., Ed.; CRC Press: Boca Raton, FL, 1991; pp 247–264.

**Figure 1.** Cutoff models for reactants and products.**Table 1.** Force Constants and Geometric Parameters for the Cutoff Model of Benzyl Alcohol Shown in Figure 1

coordinate type	atoms involved	force constant <sup>a</sup>	geometry
stretch	C2–O1	5.24	1.43 Å
stretch	C2–H3	4.78	1.10 Å
stretch	C2–H4	4.78	1.10 Å
stretch	C2–C5	4.62	1.54 Å
in-plane bend	H3–C2–C5	0.62	109.3°
in-plane bend	H4–C2–C5	0.62	109.3°
in-plane bend	H3–C2–O1	0.67	107.6°
in-plane bend	H4–C2–O1	0.67	107.6°
in-plane bend	C5–C2–O1	1.00	113.3°
in-plane bend	H3–C2–H4	0.55	109.6°

<sup>a</sup> Force constants are in units of mdyn/Å. Force constants for bending vibrations are in (mdyn Å)/rad<sup>2</sup>.

characteristics of the system.<sup>38</sup> These “cutoff” models can simplify both the actual computation and interpretation of such isotope effects. For our purposes, cutoff models of reactants, products, and transition states were used and are shown in Figure 1. These cutoff models are similar to cutoff models used by Huskey and Schowen, who showed that full and cutoff models for this reaction give comparable results.<sup>26,32,39</sup>

Vibrational frequencies were obtained by developing vibrational force fields for each of the molecules of interest. Reactant and product force constants were assigned by comparison to empirical force fields of the molecules of interest or similar molecules.<sup>40</sup> Force fields for reactants and products are shown in Tables 1–4. Force fields were fully redundant, employed internal coordinates and were diagonal in the internal coordinates (so-called simple valence force fields). Reactant and product force fields were checked for self-consistency by calculating equilibrium isotope effects using the Bigeleisen–Mayer equation. The calculated and experimental equilibrium isotope effects are shown in Table 5.

(37) Sims, L. B.; Lewis, D. E. Bond Order Methods for Calculating Isotope Effects in Organic Reactions. In *Isotope Effects: Recent Developments in Theory and Experiment*; Buncl, E., Lee, C. C., Ed.; Elsevier: New York, 1984; Vol. 6, pp 161–259.

(38) Stern, M. J.; Wolfsberg, M. *J. Chem. Phys.* **1966**, *45*, 4105–4124.

**Table 2.** Force Constants and Geometric Parameters for the Cutoff Model of Benzaldehyde Shown in Figure 1 (See Table 1 for Units)

coordinate type	atoms involved	force constant	geometry
stretch	H1–C2	4.24	1.09 Å
stretch	O3–C2	12.4	1.24 Å
stretch	C4–C2	4.68	1.48 Å
in-plane bend	H1–C2–O3	0.81	120.0°
in-plane bend	H1–C2–C4	0.44	115.0°
in-plane bend	O3–C2–C4	1.10	125.0°
out-of-plane bend	H1–(O3–C2–C4)	0.36	0.0°

**Table 3.** Force Constants and Geometric Parameters for NAD<sup>+</sup> for the Cutoff Model of NAD<sup>+</sup> Shown in Figure 1 (See Table 1 for Units)

coordinate type	atoms involved	force constant	geometry
stretch	C1–H2	5.212	1.08 Å
stretch	C1–C3	6.21	1.40 Å
stretch	C1–C4	6.21	1.40 Å
in-plane bend	H2–C1–C3	0.48	121.0°
in-plane bend	H2–C1–C4	0.48	121.0°
in-plane bend	C3–C1–C4	0.93	118.0°
out-of-plane bend	H2–(C3–C1–C4)	0.27	0.0°

**Table 4.** Force Constants and Geometric Parameters for NADH for the Cutoff Model in Figure 1 (See Table 1 for Units)

coordinate type	atoms involved	force constant	geometry
stretch	C1–H2	4.571	1.09 Å
stretch	C1–H3	4.571	1.09 Å
stretch	C1–C4	4.761	1.52 Å
stretch	C1–C5	4.761	1.52 Å
in-plane bend	H2–C1–C4	0.62	110.2°
in-plane bend	H2–C1–C5	0.62	110.2°
in-plane bend	H3–C1–C4	0.62	110.2°
in-plane bend	H3–C1–C5	0.62	110.2°
in-plane bend	C4–C1–C5	1.34	110.7°
in-plane bend	H2–C1–H3	0.59	105.0°

**Table 5.** Comparison of Calculated and Measured Equilibrium Isotope Effects<sup>a</sup>

	equilibrium	lit.	calcd
benzyl alcohol → benzaldehyde (α-secondary deuterium)		1.26 <sup>71</sup>	1.23
benzyl alcohol → benzaldehyde (α-secondary tritium)		1.33 <sup>45</sup>	1.33
NAD <sup>+</sup> → NADH (α-secondary deuterium)		0.887 <sup>71</sup>	0.895
benzyl alcohol → NADH (primary deuterium)		1.069 <sup>71</sup>	1.037
benzyl alcohol → benzaldehyde (primary carbon)		0.9847 <sup>56</sup>	0.987

<sup>a</sup> The experimental equilibrium isotope effects are from published data. The calculated equilibrium isotope effects are generated using the Bigeleisen–Mayer equation and the force constants and geometric parameters given in Tables 1–4. See text for details.

Transition state internal coordinates are shown in Figure 2. Most geometric parameters and diagonal force constants in the transition state were assigned as a weighted average of reactant and product parameters which can be represented numerically as

$$A_{is} = A_p \mathbf{X} + A_r (1 - \mathbf{X}) \quad (6)$$

where  $A$  denotes reactant ( $A_r$ ), product ( $A_p$ ), or transition state ( $A_{is}$ ) force constants or geometric parameters and  $\mathbf{X}$  represents the progress of the transition state toward product.<sup>37,39</sup> Primary hydrogen bond lengths were assigned using the Pauling equation assuming that bond order is conserved around the reacting hydrogen. Linear bending coordinates (23 and 24 in Figure 2) were assigned using the method given by Huskey.<sup>39</sup>

A force field with only diagonal force constants will not generate any motion corresponding to the transfer of the hydrogen from donor to acceptor, the reaction coordinate. The reaction coordinate is, by

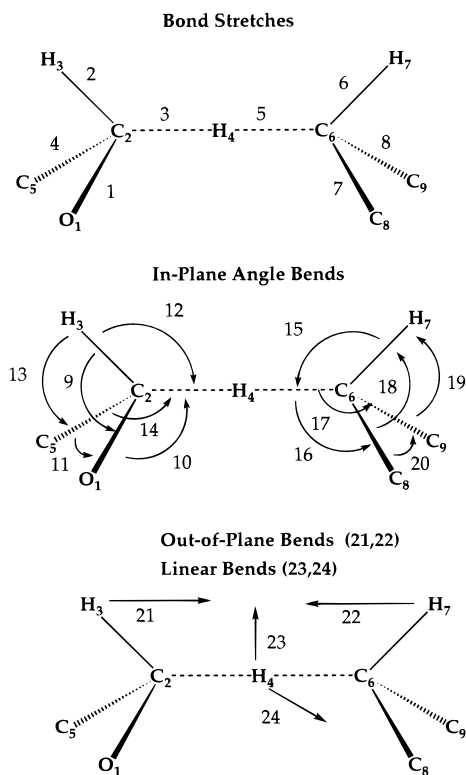


Figure 2. Internal coordinates for ADH transition state structures.

definition, the unique unstable vibration which occurs at the transition state. Reaction coordinate motion was generated by coupling internal coordinates together using off-diagonal force constants in the vibrational force field. If correctly chosen, off-diagonal force constants will generate an imaginary frequency which corresponds to the reaction coordinate.<sup>37</sup>

Tunneling was included by use of the truncated Bell correction.<sup>8</sup> The Bell correction was derived for the tunneling of a Boltzmann distribution of particles through a truncated parabolic potential barrier defined by its reaction coordinate frequency (barrier curvature),  $\nu^\ddagger$ , and barrier height,  $E$ . The Bell correction is often truncated after its first term, which corresponds to correcting for tunneling near the top of a parabolic barrier. The truncated Bell correction is of the form

$$Q = \frac{(u/2)}{\sin(u/2)} \quad (7)$$

where  $Q$  is the tunnel correction and

$$u = h\nu^\ddagger/kT \quad (8)$$

where  $\nu^\ddagger$  is the reaction coordinate frequency,  $h$  is Planck's constant,  $k$  is the Boltzmann constant, and  $T$  is the temperature. The advantage of the truncated Bell correction is that it is only dependent on the reaction coordinate frequency of the transition state. The tunnel correction to an isotope effect,  $(k_H/k_T)$ , is given as

$$\left(\frac{k_H}{k_T}\right)_{\text{full}} = \left(\frac{Q_H}{Q_T}\right)\left(\frac{k_H}{k_T}\right)_{\text{SC}} \quad (9)$$

where  $(k_H/k_T)_{\text{full}}$  is the actual isotope effect,  $(Q_H/Q_T)$  is the tunnel correction to the isotope effect, and  $(k_H/k_T)_{\text{SC}}$  is the semiclassical isotope effect calculated by vibrational analysis and the Bigeleisen–Mayer equation.  $Q_H$  and  $Q_T$  are tunnel corrections for H and T substituted

(39) Huskey, W. P. Expression of the thermal adaptation of bacteria in the mechanism of lactate dehydrogenase action: experimental isotope effects and related theoretical studies. Ph.D. Dissertation, University of Kansas, 1985.

(40) Rucker, J. B. Probes of hydrogen tunneling in enzyme-catalyzed reactions. University of California, Berkeley, CA, 1995.

transition states. The truncated Bell correction has been used by many researchers and gives results comparable to other simple tunnel corrections.

Modeling of isotope effects was accomplished by first choosing a transition state position and assigning all geometrical and force field parameters using the appropriate equations. Interactive parameters were then added to produce a reasonable reaction coordinate frequency (imaginary frequency) and isotope effects calculated using the Bigeleisen–Mayer equation, the truncated Bell correction (eq 7), and eq 9. Interactive force constants were then adjusted in such a way as to reproduce the experimental  $^1(k_H/k_T)_H$  and  $^2(k_H/k_T)_H$  isotope effects (7.13 and 1.35).<sup>2</sup> At this point, the calculated  $^1(k_D/k_T)_D$  and  $^2(k_D/k_T)_D$  were examined and compared to the experimental values of 1.73 and 1.03, respectively. If the agreement was unsatisfactory, either interactive force constants or the transition state position were changed so as to get the best fit to the experimental data. This method is basically a trial and error approach, although chemical and mathematical intuition were quite helpful. There is also a more rational approach called the curvature parameter method.<sup>41</sup> However, it is extremely cumbersome to use for complicated systems and was not used in the present study.

All calculations were done on either a Macintosh SE/30 or Powerbook 180c using the program BEBOVIB IV.<sup>42</sup> This program solves the vibrational secular equations for the molecules of interest using user-derived force fields. The program then calculates isotope effects using the calculated vibrational frequencies and the Bigeleisen equation.

## Results and Discussion

**Transition State Structure.** Much is already known about the transition state structure for YADH. Structure–reactivity analyses of both para-substituted benzyl alcohols and benzaldehydes suggest that the transition state for the YADH-catalyzed reaction is quite alcohol-like.<sup>43–45</sup> In these earlier studies,  $k_{\text{cat}}$  for benzyl alcohol oxidation was shown to be independent of electronic effects while  $k_{\text{cat}}$  for benzaldehyde oxidation was strongly dependent on electronic substituent effects. These results imply an alcohol-like transition state electronic structure. The small  $^2(k_D/k_T)_D$  isotope effect (which should be free of complications due to kinetic complexity) in the YADH system also suggested an early transition state.<sup>2</sup> Finally, Tapia and co-workers performed ab initio calculations on the transition state for the transfer of a hydrogen from methanolate anion to pyridinium cation which give alcohol-like transition state geometries.<sup>46,48</sup>

In terms of the geometry of the transition state, there is evidence that hydrogen transfer in the ADH reaction should be linear. The observed binding of pentafluorobenzyl alcohol in the crystal structure of HLADH indicates that the pro-R hydrogen of substrate points almost directly toward the acceptor carbon of NAD<sup>+</sup>.<sup>49</sup> The position of a pro-R hydrogen on C4 of an NADH modeled into the active site is about 40° displaced from the vector between the alcohol pro-R hydrogen and C4 of NAD<sup>+</sup>. Thus one would expect the donor–hydrogen–acceptor angle in the transition state to be somewhere between 140° and 180°, essentially linear. Both ab initio and semiempirical calculations of hydride transfer reactions also support the idea

(41) Buddenbaum, W. E.; Yankwich, P. E. *J. Phys. Chem.* **1967**, *71*, 3136–3143.

(42) Sims, L. B.; Burton, G.; Lewis, D. E.; *Bebovib IV*, Program No. 337; Quantum Chemistry Program Exchange; Department of Chemistry, Indiana University: Bloomington, IN, 1977.

(43) Klinman, J. P. *J. Biol. Chem.* **1972**, *247*, 7977–7987.

(44) Klinman, J. P. *Biochemistry* **1976**, *15*, 2018–2026.

(45) Welsh, K. M.; Creighton, D. J.; Klinman, J. P. *Biochemistry* **1980**, *19*, 2005–2016.

(46) Tapia, O. *J. Mol. Catal.* **1988**, *47*, 199–210.

that the angle of hydride transfer in the transition state will fall within this range.<sup>49–54</sup>

Considering this information, we will limit our study to early transition states with  $\mathbf{X}$  equal to 0.1–0.3. In addition, only linear transition states with  $\theta(\text{C}_{\text{alc}}\text{HC}_{\text{NAD}^+})$  equal to  $180^\circ$  will be considered. The assumption of a linear transition state suggests that torsional motion around the hydrogen transfer coordinate (C2–H4–C6) in the transition state will have a force constant of zero.<sup>37,39</sup>

**Coupled Motion and Tunneling Can Reproduce Some of the Experimental Isotope Effects.** A transition state reaction coordinate is generated by including interactive force constants between vibrational modes in the transition state force constant matrix. A reasonable first model is one which includes only interactive force constants between the primary hydrogen stretching motion and motion of the secondary hydrogen on the alcohol in addition to the coupling between the two primary carbon–hydrogen stretching modes. There are three internal coordinates which include the motion of the secondary hydrogen: the secondary hydrogen stretch ( $F_2$ ), the in-plane bending motion involving the two hydrogens ( $F_{12}$ ), or the out-of-plane hydrogen bending mode ( $F_{21}$ ). Intuitively, one would expect rehybridization to look like an umbrella-bending motion ( $F_{21}$ ). This means that for any particular transition state position, the stretch–stretch interaction,  $f_{3,5}$ , and the alcohol stretch–bend interaction,  $f_{3,21}$  will need to be determined. The phase of the interactions is also important, with a negative interactive force constant indicating that the two internal coordinates are moving in-phase with each other and a positive interactive force constant indicating that the two internal coordinates are  $180^\circ$  out-of-phase.

However, this simple model, not unexpectedly, failed to reproduce the observed isotope effects (data not shown). To a large degree, this is due to a lack of stretch–bend cofactor coupling, since it is known that rehybridization of the C4 carbon on  $\text{NAD}^+$  is also a part of the reaction coordinate. For example, the observed  $\text{NAD}^+$   $\alpha$ -secondary isotope effect for YADH with 2-propanol is 1.08, with an estimated intrinsic effect of 1.22, implying substantial hydrogenic motion in the transition state.<sup>55</sup>

Can better agreement with experimental values be systematically obtained using three interactive force constants? Consider a series of models at a transition state position of 0.1. Each model has three interactive force constants: stretch–stretch ( $f_{3,5}$ ), alcohol stretch–bend ( $f_{3,21}$ ), and cofactor stretch–bend ( $f_{5,22}$ ). Modeling with two force constants demonstrated that a given pair of ( $k_{\text{H}}/k_{\text{T}}$ ) isotope effects can be generated by a unique pair of interactive force constants. By choosing an arbitrary cofactor stretch–bend ( $f_{5,22}$ ), a unique pair of the remaining interactive force constants can be determined using the previously discussed procedure. A series of these calculations is shown in Table 6. As the cofactor interactive force constant gets larger, the reaction coordinate frequency increases and thus the amount of tunneling

**Table 6.** Models with Three Interactive Force Constants<sup>a</sup>

$f_{5,22}$	$\nu^\ddagger$ ( $\text{i cm}^{-1}$ )	$1^\circ$ exponent	$2^\circ$ exponent	$2^\circ$ ( $k_{\text{H}}/k_{\text{D}}$ ) for $\text{NAD}^+$	( $k_{12\text{C}}/k_{13\text{C}}$ ) <sub>H</sub>
0.4	−981.6	3.48	5.37	1.042	1.021
0.6	−1073.2	3.51	5.76	1.14	1.020
0.8	−1148.2	3.55	6.34	1.35	1.017

<sup>a</sup> Isotope effects were generated using transition states where the stretch–bend coupling between the cofactor and the primary hydrogen was systematically increased. The primary hydrogen stretch–stretch coupling and the stretch–bend coupling between alcohol and the primary hydrogen were then adjusted to reproduce the experimental  $1^\circ$  ( $k_{\text{H}}/k_{\text{T}}$ )<sub>H</sub> and  $2^\circ$  ( $k_{\text{H}}/k_{\text{T}}$ )<sub>H</sub> values. See text for details.

increases. This increase is mirrored by an increase in the size of the exponents. As the exponents increase, so does the cofactor secondary isotope effect. The best model of the set has an  $\alpha$ -secondary deuterium isotope effect on  $\text{NAD}^+$  of 1.35, which is almost certainly too large.

Nonetheless, this model (which is analogous to the model used by Huskey and Schowen<sup>26</sup>) does a good job of reproducing many of the experimental data. The primary exponent (and thus primary isotope effects) are within experimental error. Even more interesting is that the alcohol methylene carbon isotope effect for this model (also shown in Table 6) is identical to the experimentally measured carbon isotope effect<sup>56</sup> (carbon isotope effects will be explored in further detail in a later section). One problem with this model is that the alcohol  $2^\circ$  ( $k_{\text{D}}/k_{\text{T}}$ )<sub>D</sub> of 1.048 is still high considering the experimental value of  $1.03 \pm 0.01$ . In addition, the reaction coordinate frequency of  $-1148.21 \text{ i cm}^{-1}$  is somewhat high considering the validity of the truncated Bell correction, although it is a reasonable value considering frequencies from ab initio calculations of hydride transfer reaction.<sup>49,51,54</sup>

**$2^\circ$  ( $k_{\text{D}}/k_{\text{T}}$ )<sub>D</sub> Variation and the Reaction Coordinate Eigenvector.** The models utilizing simple coupling between the primary and secondary hydrogens reproduce the data extremely well. However, the computed values for  $2^\circ$  ( $k_{\text{D}}/k_{\text{T}}$ )<sub>D</sub> isotope effects are too large given a  $2^\circ$  ( $k_{\text{H}}/k_{\text{T}}$ )<sub>H</sub> of 1.35 for alcohol. What is the possible origin of this effect? The exponents that were measured by Cha were generally of the form given by eq 3. As mentioned previously,  $y$  is a combination of two effects, a pure Swain–Schaad exponent,  $s$ , and an RGM deviation,  $r$ , where Huskey has shown that RGM deviations can be a major component of  $y$ .<sup>32</sup> The tunnel correction to an isotope effect generally increases with the reaction coordinate frequency. Any perturbation which lowers the reaction coordinate frequency will lower the tunneling contribution to the isotope effect. For example, consider our model where  $2^\circ$  ( $k_{\text{H}}/k_{\text{T}}$ )<sub>H</sub> is 1.35 and the reaction coordinate frequency is  $-982 \text{ i cm}^{-1}$ . Deuterium substitution in the primary position lowers the reaction coordinate frequency to  $-865.5 \text{ i cm}^{-1}$ . Consequently, this gives a  $2^\circ$  ( $k_{\text{H}}/k_{\text{T}}$ )<sub>D</sub> of 1.16. Likewise, the  $2^\circ$  ( $k_{\text{D}}/k_{\text{T}}$ )<sub>H</sub> goes from 1.11 to 1.058 upon deuterium substitution in the primary position. Primary isotope effects show a similar, but smaller, effect upon secondary substitution. We note that there is almost no RGM breakdown in these models without the inclusion of a tunnel correction (data not shown). A reduction in secondary isotope effect upon deuteration in the primary position has been seen experimentally in the enzymatic systems of glucose-6-phosphate dehydrogenase and formate dehydrogenase.<sup>29,30</sup>

In an effort to model the  $2^\circ$  ( $k_{\text{D}}/k_{\text{T}}$ )<sub>D</sub>, we examined ways to obtain larger RGM deviations between isotope effects, rather

(47) Tapia, O.; Cardenas, R.; Andres, J.; Krechl, J.; Campillo, M.; Colonna-Cesari, F. *Int. J. Quantum Chem.* **1991**, *39*, 767–786.

(48) Ramaswamy, S.; Eklund, H.; Plapp, B. V. *Biochemistry* **1994**, *33*, 5230–5237.

(49) Wu, Y.-D.; Houk, K. N. *J. Am. Chem. Soc.* **1987**, *109*, 906–908.

(50) Wu, Y.-D.; and Houk, K. N. *J. Am. Chem. Soc.* **1987**, *109*, 2226–2227.

(51) Tapia, O.; Cardenas, R.; Andres, J.; Colonna-Cesari, F. *J. Am. Chem. Soc.* **1988**, *110*, 4046–4047.

(52) Tapia, O.; Andres, J.; Cardenas, R. *Chem. Phys. Lett.* **1992**, *189*, 395–400.

(53) Cummins, P. L.; Gready, J. E. *J. Comput. Chem.* **1990**, *11*, 791–804.

(54) Williams, I. H.; Miller, A. B.; Maggiora, G. M. *J. Am. Chem. Soc.* **1990**, *112*, 530–537.

(55) Cook, P. F.; Oppenheimer, N. J.; and Cleland, W. W. *Biochemistry* **1981**, *20*, 1817–1825.

(56) Schnarschmidt, M.; Fisher, M. A.; Cleland, W. W. *Biochemistry* **1984**, *23*, 5471–5478.

**Table 7.** Mass Dependence of Reaction Coordinate Frequencies<sup>a</sup>

model	$\nu^*(\text{H,H})$	$\nu^*(\text{D,H})$	$\nu^*(\text{H,D})$
two coupled modes	-679.9	-586.0 (-13.8)	-626.5 (-7.85)
three coupled modes (1)	-981.6	-864.8 (-11.9)	-939.9 (-4.3)
three coupled modes (2)	-1073.2	-959.8 (-10.6)	-1039.3 (-3.2)
three coupled modes (3)	-1148.2	-1043.2 (-9.1)	-1123.1 (-2.2)
multiple coupled modes	-1102.1	-950.2 (-13.8)	-1064.2 (-3.4)

<sup>a</sup> Frequencies are in  $\text{cm}^{-1}$ .  $\nu^*(\text{L,L}')$  is the reaction coordinate frequency with isotope L in the primary position and isotope L' in the secondary position. The model with two coupled modes is the best fit model using only primary stretch–stretch coupling and stretch–bend coupling between the alcohol and primary hydrogen. The three models with three coupled modes are described in Table 6. The model with many coupled modes is described in the text and in further detail in Table 8. The percent deviation from the unsubstituted frequency is shown in parentheses.

than trying to increase Swain–Schaad deviations. Phenomenologically, the systems which show the largest RGM deviations are those where isotopic substitution eliminates the largest amount of tunneling, i.e., where isotopic perturbation has the greatest effect on the reaction coordinate frequency. For substitutions in one position to affect the isotope effect in another position, the two positions need to be coupled. Unfortunately, these two requirements often work against each other. Table 7 shows the reaction coordinate frequency and its isotopic dependence for a number of different models. All of these models are ones which reproduce the primary and secondary ( $k_{\text{H}}/k_{\text{T}}$ )<sub>H</sub> isotope effects. The first model is one that couples only the primary and secondary alcohol methylene hydrogens, while the next three models couple in the cofactor secondary hydrogen to different extents. By focusing on the change in frequency due to primary deuterium substitution for the first three models, one sees that as the reaction coordinate frequency increases the frequency becomes less isotopically sensitive. A similar, if smaller, effect is seen upon secondary substitution. In both cases, as the amount of coupled motion increases, the isotope dependence of the reaction coordinate decreases even though the magnitude of the frequency increases. An increase in the amount of tunneling by coupling in other coordinates decreases the isotope dependence of the reaction coordinate frequency, thus reducing the magnitude of the RGM breakdown. Almost paradoxically, coupled motion can both increase and decrease RGM deviations.

Examination of the reaction coordinate eigenvectors for these highly coupled models shows that there is a great deal of heavy-atom motion, probably as a consequence of the hydrogenic umbrella modes. This suggests that a potential origin for the decrease in isotopic sensitivity is the increase in heavy-atom motion. Is there anyway to (empirically) counteract this effect? One possibility is to couple in other internal coordinates in such a way as to cancel out the heavy-atom motion in the reaction coordinate. By looking at the reaction coordinate eigenvector and at the direction of heavy-atom motion in the reaction coordinate, one can choose appropriate internal coordinates to couple into the reaction coordinate in such a way as to cancel out heavy-atom motion. The additional interactive force constants that give the best result are  $f_{3,10}$ ,  $f_{3,14}$ ,  $f_{5,16}$ , and  $f_{5,17}$ . These correspond to stretch–bend interactions with both oxygen and carbon in-plane bending coordinates. By a combination of intuition and trial and error, better modeling of the observed isotope effects is obtained. The last entry of Table 7 shows the mass dependence of the reaction coordinate frequency for a model with many coupled modes. Both the primary and secondary isotope effects on the reaction coordinate frequency show a greater mass dependence than the models with only three coupled modes, although the absolute magnitude of the reaction

**Table 8.** Reasonable Model for a Transition State<sup>a</sup>

isotope effect	exptl	calcd (full)	calcd (SC)
$^{1^\circ}(k_{\text{H}}/k_{\text{T}})_{\text{H}}$	$7.13 \pm 0.07$	7.14	3.02
$^{1^\circ}(k_{\text{D}}/k_{\text{T}})_{\text{D}}$	$1.73 \pm 0.02$	1.70	1.39
$^{2^\circ}(k_{\text{H}}/k_{\text{T}})_{\text{H}}$	$1.35 \pm 0.02$	1.35	1.014
$^{2^\circ}(k_{\text{D}}/k_{\text{T}})_{\text{D}}$	$1.03 \pm 0.01$	1.04	1.004
$^{1^\circ}(k_{\text{H}}/k_{\text{T}})_{\text{D}}$		6.07	3.00
$^{1^\circ}(k_{\text{D}}/k_{\text{T}})_{\text{H}}$		1.75	1.39
$^{2^\circ}(k_{\text{H}}/k_{\text{T}})_{\text{D}}$		1.12	1.007
$^{2^\circ}(k_{\text{D}}/k_{\text{T}})_{\text{H}}$		1.10	1.006

<sup>a</sup> This is a model with many coupled modes that gives good agreement with experimental isotope effects. This is an early transition state ( $x = 0.1$ ) with the following interactive force constants:  $f_{3,5} = 1.366$ ,  $f_{3,21} = -0.616$ ,  $f_{5,22} = 0.80$ ,  $f_{3,10} = 0.6$ ,  $f_{3,14} = 0.6$ ,  $f_{5,16} = -0.6$ ,  $f_{5,17} = -0.6$ .

coordinate frequency shows that there is a great deal of coupling. This is the model that reproduced the observed isotope effects to the greatest degree.

As an alternative, we considered the possibility that torsional motion around the  $\text{C}\alpha\text{--C}\beta$  axis of alcohol (C2–C5) might contribute to secondary isotope effects and allow for a better match with the experimental data. Exploration of the effect of torsional motion required the addition of two additional carbon atoms to the model, as well as stretching and bending force constants for the additional internal coordinates generated. Force constants for torsional motion around  $\text{C}\alpha\text{--C}\beta$  bonds in alcohols and aldehydes are generally quite small and similar in magnitude, which suggests that there should be a negligible torsional force constant difference between reactant alcohol and the transition state. Models which included only small differences between reactant and transition state torsional force constants showed essentially no difference from the previous model (data not shown). However, a model in which the transition state torsional mode is much stiffer than the reactant torsional mode, showed inflated exponents for both primary and secondary isotope effects. Interestingly, this model shared many properties with the previous model. In particular, it generated reaction coordinate motion with increased isotopic sensitivity. For the remainder of this section we will explicitly discuss the model with many-coupled modes although a transition state with similar properties can also be generated by modulation of alcohol torsional motion.

Table 8 tabulates both experimental and calculated primary and secondary isotope effects for the YADH-catalyzed oxidation of benzyl alcohol. The agreement is quite good with the calculated values being within a standard deviation of the observed values. In addition, the calculated  $^{2^\circ}(k_{\text{H}}/k_{\text{D}})_{\text{NAD}^+}$  isotope effect of 1.28 nicely agrees with the intrinsic isotope effect of 1.22 as estimated by Cook et al.<sup>55</sup> It should, once again, be noted that, except for  $^{2^\circ}(k_{\text{D}}/k_{\text{T}})_{\text{D}}$ , the other measured hydrogen isotope effects can be well reproduced by a simple model with only three coupled modes. Although reproducing these values requires coupled motion and tunneling, they are *much less* sensitive to the specifics of transition state structure than  $^{2^\circ}(k_{\text{D}}/k_{\text{T}})_{\text{D}}$ .

Table 8 also shows semiclassical isotope effects (SC) for the reaction. It is obvious that there is a large contribution of tunneling to primary isotope effects with the tunnel correction increasing  $^{1^\circ}(k_{\text{H}}/k_{\text{T}})_{\text{H}}$  by over 100% with respect to its semiclassical value. Even the  $^{1^\circ}(k_{\text{D}}/k_{\text{T}})_{\text{D}}$  effect shows a substantial tunnel effect. Both primary and secondary semiclassical isotope effects adhere to Swain–Schaad and RGM behavior. As per the modeling work of Huskey, most of the magnitude of  $\gamma$  for secondary isotope effects is due to RGM deviations,  $r$ , not Swain–Schaad deviations,  $s$ .<sup>32</sup> The magnitude of  $\gamma$  for primary

isotope effects is mostly due to Swain–Shaad deviations with some contribution from RGM breakdown. However, the RGM breakdown of  $^{10}(k_{\text{H}}/k_{\text{T}})_{\text{H}}$  upon deuteration of the secondary hydrogen is quite large (from 7.14 to 6.07). All of this is consistent with previous studies.

In contrast, comparison of the full and SC secondary isotope effects shows that, for this model, the secondary isotope effects are primarily quantum mechanical. This may have important consequences for the interpretation of secondary isotope effects in related systems. Semiclassical secondary isotope effects are considered to be indicators of transition state geometry in certain types of reactions, e.g., rehybridization.<sup>55,57</sup> This is generally interpreted as meaning that kinetic secondary isotope effects should range between unity and the equilibrium isotope effect.<sup>37,58</sup> A transition state position of 0.1 implies a semiclassical secondary  $(k_{\text{H}}/k_{\text{T}})$  isotope effect of approximately 1.03–1.04, assuming a linear relation between transition state position and secondary isotope effect. As pointed out by Klinman, coupled motion can increase semiclassical secondary isotope effects.<sup>16</sup> In a system with coupled motion between primary and secondary hydrogens, one would expect a semiclassical  $^{20}(k_{\text{H}}/k_{\text{T}})_{\text{H}}$  effect of greater than 1.04.

However, in the case that coupled motion gets very large, the semiclassical contribution to the secondary isotope effect can be suppressed. Coupling between internal modes can raise the frequency of vibrational modes orthogonal to the reaction coordinate which can lower the isotope effect. In such a case, the secondary hydrogen can look “tighter” due to coupled motion. As calculated in this model, the semiclassical secondary  $(k_{\text{H}}/k_{\text{T}})$  effect is 1.014, almost unity; the semiclassical  $^{20}(k_{\text{H}}/k_{\text{T}})_{\text{H}}$  and  $^{20}(k_{\text{D}}/k_{\text{T}})_{\text{D}}$  effects are much smaller (earlier) than the transition state position would suggest. In a compensatory fashion, tunneling effectively magnifies the reaction coordinate contribution to an observed isotope effect. With tunneling, the  $^{20}(k_{\text{H}}/k_{\text{T}})_{\text{H}}$  is inflated to the equilibrium limit (1.33). The  $^{20}(k_{\text{D}}/k_{\text{T}})_{\text{D}}$  looks much smaller than the equilibrium limit (1.1) because the deuterium in the primary position reduces tunneling and thus the isotope effect. Since tunneling is the origin of much of the isotope effect, including  $^{20}(k_{\text{D}}/k_{\text{T}})_{\text{D}}$ , this comparison between equilibrium and kinetic secondary isotope effects is ambiguous; the secondary equilibrium isotope effect probes changes in bonding, while the secondary kinetic isotope effect in this model probes the mass dependence of the reaction coordinate frequency. The inclusion of coupled motion and tunneling in this model causes a loss of information about transition state structure. What is gained is detailed information about the reaction coordinate.

Even though this model is quite good, particularly with respect to the isotope effects at 25 °C, there are a number of problems associated with it. The carbon isotope effect calculated for this model (1.0293) does not agree with the experimentally measured carbon isotope effect<sup>56</sup> as well as the model with only three coupled modes. However, we suspect that this discrepancy could easily be resolved with additional modifications to the current model. The transition state position is earlier than one would expect from ab initio calculations of model hydride transfers. Finally, the temperature dependence of the calculated  $^{10}(k_{\text{H}}/k_{\text{T}})_{\text{H}}$  isotope effect is much steeper than seen experimentally (data not shown). Although there is good evidence for a single rate-limiting step in the YADH-catalyzed oxidation of benzyl alcohol at 25 °C,<sup>43</sup> it seems likely that kinetic complexity

increases as the temperature is lowered.<sup>59</sup> Such an effect would flatten out the experimental plot of the  $\ln(\text{isotope effect})$  versus  $1/T$  in relation to the calculated data points.

Probably the major source of error in these calculations is the determination of transition state force constants. It is assumed that transition state force constants can be interpolated from ground state force constants using the methods outlined. In such cases, force constants would range from reactant-like values for early transition states to product-like values for late transition states. One would expect the transition state force constants to mirror the transition state properties as determined from other methods such as structure–reactivity correlations. However, there is no intrinsic reason for this to be true, especially considering the influence of coupled motion and tunneling. Ab initio calculations of isotope effects for a series of E2 model systems showed the relationship between kinetic isotope effects and transition state structure to be much more complicated than expected from standard physical organic principles.<sup>60</sup> One could say that the transition state force constants are influenced by resonance structures that are unimportant in the ground state. Importantly, even though certain aspects of the transition state structure might be incorrect, the calculations described herein lead to a single model which is able to reproduce the currently available hydrogen isotope effects in the YADH system.

### Carbon Isotope Effects

During the course of these computations, some interesting observations regarding carbon isotope effects at the methylenic carbon of benzyl alcohol were noticed. Carbon isotope effects have been measured by Cleland and co-workers for a variety of enzyme systems.<sup>29,30,56</sup> In these studies,  $^{12}\text{C}/^{13}\text{C}$  isotope effects with both protium and deuterium as the transferred particle were measured. The change in carbon isotope effect was then used to determine the amount of kinetic complexity present in a particular reaction.<sup>36</sup> The main assumption of this type of analysis is that carbon isotope effects and hydrogen isotope effects, on any single kinetic step, are independent of one another, i.e., that the rule of the geometric mean between these two isotope effects is valid.

Of particular interest are the carbon isotope effects for the YADH and HLADH reactions. As a frame of reference, the experimental  $^{12}\text{C}/^{13}\text{C}$  equilibrium isotope effect going between benzyl alcohol and benzaldehyde is  $0.9847 \pm 0.0005$ .<sup>56</sup> Using the force constants for benzyl alcohol (Table 1) and benzaldehyde (Table 2) one calculates a  $^{12}\text{C}/^{13}\text{C}$  equilibrium isotope effect of 0.987. The kinetic carbon isotope effects ( $^{13}(\text{V}/\text{K})_{\text{H}}$  and  $^{13}(\text{V}/\text{K})_{\text{D}}$ ) for the two ADHs are quite similar: 1.015–1.016 when H is the transferred particle and 1.022 when D is the transferred particle. Cleland and co-workers have argued that this difference is due to kinetic complexity under the reactions conditions used. Such kinetic complexity, which diminishes the size of the observed carbon isotope effect when protium is transferred, is reduced when C–D is cleaved, leading to a corresponding increase in the observed  $^{12}\text{C}/^{13}\text{C}$  effect. However, there is strong evidence that hydrogen transfer is fully rate-limiting in YADH with para-substituted benzyl alcohols as substrates.<sup>43,44</sup> The fact that large Swain–Schaad deviations are seen in this system is also good evidence that hydrogen transfer is almost fully rate-limiting.<sup>2,61</sup>

Can we assume that this rule of the geometric mean is held when isotopic substitutions are made at adjacent hydrogen–

(57) Streitwieser, A.; Jagow, R. H.; Fahey, R. C.; and Suzuki, S. *J. Am. Chem. Soc.* **1984**, *106*, 2326–2332.

(58) Klinman, J. P. *Adv. Enzymol.* **1978**, *415*–454.

(59) Tsai, S.; Klinman, J. P. Unpublished data.

(60) Jensen, F.; Glad, S. S. *J. Am. Chem. Soc.* **1994**, *116*, 9302–9310.

(61) Rucker, J.; Cha, Y.; Jonsson, T.; Grant, K. L.; Klinman, J. P. *Biochemistry* **1992**, *31*, 11489–11499.



**Table 9.** Calculated Carbon Isotope Effects (Carbon Isotope Effects Were Calculated for the Same Models as Described in Table 7)

model	$(^{12}\text{C}/^{13}\text{C})_{\text{H}}$ (SC)	$(^{12}\text{C}/^{13}\text{C})_{\text{D}}$ (SC)	$(^{12}\text{C}/^{13}\text{C})_{\text{H}}$ (full)	$(^{12}\text{C}/^{13}\text{C})_{\text{D}}$ (full)
two coupled modes	1.0150	1.0217	1.0192	1.0247
three coupled modes (1)	1.0168	1.0224	1.0209	1.0249
three coupled modes (2)	1.0163	1.0218	1.0201	1.0238
three coupled modes (3)	1.0143	1.0197	1.0172	1.0208
multiple coupled modes	1.0239	1.0298	1.0293	1.0328

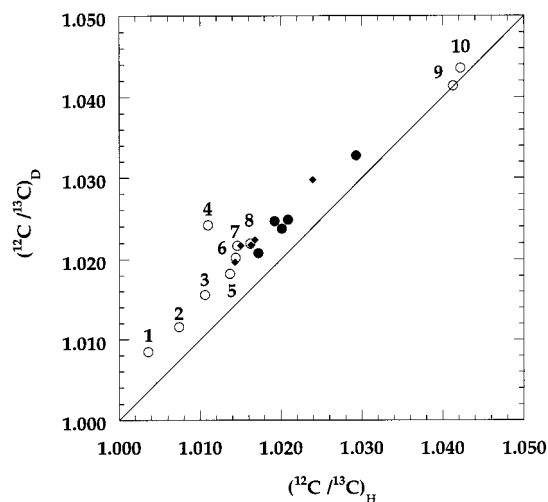


**Figure 3.** Experimental and computed heavy-atom RGM deviations. Calculated values are shown in Table 9. Experimental values are from the literature. The solid line represents the situation where the rule of the geometric mean is obeyed. (circle) Calculated semiclassical heavy-atom isotope effects. (diamond) Calculated full heavy-atom isotope effects. (open circle) Experimental heavy-atom isotope effects. 1: HLADH/benzyl alcohol/acetylpyridine-NAD<sup>+</sup>.<sup>56</sup> 2: HLADH/benzyl alcohol/thio-NAD<sup>+</sup>.<sup>56</sup> 3: HLADH/benzyl alcohol/pyridinealdehyde-NAD<sup>+</sup>.<sup>56</sup> 4: G6DH/glucose-6-phosphate/NAD<sup>+</sup>.<sup>30</sup> 5: HLADH/benzyl alcohol/deamino-NAD<sup>+</sup>.<sup>56</sup> 6: ALDH/benzaldehyde/NAD<sup>+</sup>.<sup>56</sup> 7: HLADH/benzyl alcohol/NAD<sup>+</sup>.<sup>56</sup> 8: YADH/benzyl alcohol/NAD<sup>+</sup>.<sup>56</sup> 9: FDH/formate/pyridinealdehyde-NAD<sup>+</sup>.<sup>29</sup> 10: FDH/formate/NAD<sup>+</sup>.<sup>29</sup>

carbon sites? Computational models show that carbon isotope effects can vary a great deal upon deuteration. In a few cases, the isotope effect is reduced upon deuteration (data not shown). This situation is analogous to RGM breakdown as seen for multiple hydrogen isotope effects: deuterium substitution decreases the tunneling contribution to the carbon isotope effect. In other cases, the carbon isotope effect increases to some extent upon deuteration. Table 9 gives the carbon isotope effects for both hydrogen and deuterium transfer using the models described above. In all cases, both full and semiclassical isotope effects show a substantial and similar increase in the semiclassical carbon isotope effect upon deuteration. Models that include alcohol torsional motion also show this behavior, although the effect is masked by tunneling (though not eliminated) in the model where torsional motion is much stiffer in the transition state (data not shown). As noted in the preceding section, a model of this extreme nature is considered unlikely. In Figure 3, the  $^{12}\text{C}/^{13}\text{C}$  isotope effect for deuterium transfer is plotted versus  $^{12}\text{C}/^{13}\text{C}$  for hydrogen transfer using both experimental and computational data points. It can be seen that most of the points deviate from RGM behavior (represented by the solid line) in a similar manner. Also included on this graph are  $^{13}\text{C}/^{12}\text{C}_{\text{H}}$  and  $^{13}\text{C}/^{12}\text{C}_{\text{D}}$  isotope effects for HLADH and FDH with a variety of cofactors. Similar behavior of semiclassical isotope effects has been seen by Saunders in his computational studies of elimination reactions, although its relevance to studies of

kinetic complexity was not noted.<sup>1</sup> Thus, these deviations do not appear to be caused by the specific coupling schemes in the ADH computational models.

The rule of the geometric mean is generally considered to be an empirical relationship. Bigeleisen put the rule on a firmer theoretical basis, the RGM being a consequence of the isotopic sum rule<sup>62</sup> combined with certain approximations to the Bigeleisen–Mayer equation.<sup>5,24,63</sup> However, the RGM is only an approximation. Bigeleisen and Ishida examined deviations from the RGM for small molecule systems.<sup>25</sup> Although they did not examine deviations in the case of mixed isotopic substitutions, they did examine deviations for multiple hydrogen substitutions and multiple carbon isotope substitutions. The latter case is relevant to the current discussion. They examined RGM deviations in the disproportionation of [ $^{13}\text{C}_2$ ]ethylene and [ $^{12}\text{C}_2$ ]ethylene to form [ $^{13}\text{C}^{12}\text{C}$ ]ethylene. What they noticed is that the largest component of the RGM deviation was due to the carbon–carbon stretching motion, the molecular motion which most involves the motion of the two carbon atoms. This is analogous to the proposition that RGM breakdown in the hydrogen transfer systems is largely due to the carbon–hydrogen stretching motion, the molecular motion which most involves the motion of the two atoms of interest.

We end with a caveat regarding future applications of Cleland's multiple isotope effect method. To begin with, the type of effects described here only refer to systems in which the same reacting center is labeled with both the heavy and light isotope. When a remote heavy atom isotope effect is examined as a function of deuteration,<sup>64–66</sup> the conclusions regarding kinetic or chemical complexity appear sound. However, the rule of the geometric mean cannot be assumed for hydrogen abstraction reactions where both labels are at the site of the bond cleavage. Both semiclassical considerations and tunneling can lead to (compensating) deviations from the RGM. Under certain circumstances, small changes in transition state structure might lead to significant changes in RGM deviation. As the tunneling contribution to a primary carbon isotope effect increases, the RGM deviation can potentially go from inverse (increase upon deuteration) to normal (decrease upon deuteration). Although these types of results can also be representative of changes in kinetic mechanism, properly controlled experiments/calculations are needed to rule out intrinsic effects arising from double labeling.

## Conclusions

The primary conclusion of this study regards the interpretation of secondary hydrogen isotope effects. Within the semiclassical theory of isotope effects, secondary isotope effects are considered to be probes of transition state position, and their magnitude has been thought to reflect the position of the transition state with respect to reactants and products. The presence of tunneling has been expected to complicate this interpretation of secondary isotope effects. To satisfactorily reproduce the secondary isotope effects experimentally seen in the YADH-catalyzed oxidation of benzyl alcohol, we required a model in which the semiclassical contribution to the secondary hydrogen isotope effect is

(62) Wilson, E. B., Jr.; Decius, J. C.; Cross, P. C. *Molecular Vibrations*; Dover Publications: New York, 1955.

(63) Bigeleisen, J. The Significance of the product and Sum Rules to isotope Fractionation Processes. In *Proceedings of the International Symposium on Isotope Separation*; Kistemaker, J., Bigeleisen, J., Nier, A. O., Eds.; Interscience Publishers Inc.: New York, 1958; pp 120–157.

(64) Karsten, W. E.; Gavva, S. R.; Park, S.-H.; Cook, P. F. *Biochemistry* **1995**, *34*, 3253–3260.

(65) Karsten, W. E.; Cook, P. F. *Biochemistry* **1994**, *33*, 2096–2103.

extremely small. The secondary isotope effect for *both* protium and deuterium transfer is primarily due to tunneling and is, thus, a probe of the nature of the reaction coordinate rather than a reflection of the transition state position. This effect seems to be due to coupled motion, which has also been implicated in increasing secondary isotope effects.<sup>17,26</sup>

Our work has also brought to light an interesting property of carbon isotope effects which appears to have not been commented on previously in the literature. Primary carbon isotope effects in hydrogen transfer reactions are inflated upon deuteration of the primary hydrogen. This effect appears to be due neither to tunneling nor to coupled motion, but rather is due to the change in reduced mass of a carbon–hydrogen bond upon deuteration. It appears that many experimentally measured primary carbon isotope effects obey this relationship. This has implications for the use of heavy-atom isotope effects as probes of reaction mechanism, where it may have been incorrectly assumed that the RGM will hold.

An obvious weakness with the modeling discussed herein is the lack of explicit inclusion of the enzyme. Isotope effects are local phenomena, probing the changes in bonding near the site of isotopic substitution. Vibrational analysis, which calculates only isotope effects, focuses exclusively on the force constants

(66) Edens, W. A.; Urbauer, J. L.; Cleland, W. W. *Biochemistry* **1997**, *36*, 1141–1147.

(67) Borgis, D.; Hynes, J. T. Proton-Transfer Reactions. In *The Enzyme Catalysis Process*; Copper, A., Houben, J. L., Chien, L. C., Eds.; Plenum Press: New York, 1989; pp 293–302.

(68) Kim, Y.; Truhlar, D. G.; Kreevoy, M. M. *J. Am. Chem. Soc.* **1991**, *113*, 7837–7847.

(69) Warshel, A.; Hwang, J. K.; Åqvist, J. *Faraday Discuss.* **1992**, *93*, 225–238.

that are near the sites of isotopic substitution. For example, in the YADH reaction, even the catalytic zinc has been ignored, since it is more than two bonds removed from the sites of isotopic substitution. More sophisticated theoretical models can include the effect of the environment on the reaction rates and isotope effects.<sup>67–69</sup> However, vibrational analysis may also be useful for probing the effects of protein structure on catalysis when the measurement and computation of isotope effects is combined with site specific mutagenesis experiments. Bahnson et al. have already examined changes in hydrogen isotope effects due to site-specific mutations in the HLADH system.<sup>34,70</sup> In an initially unanticipated manner, the experimental trends in isotope effects with HLADH mirror the computations shown here, i.e., the  $2^\circ(k_D/k_T)_D$  parameter appears as the single most sensitive indicator of changes in active site structure and catalytic efficiency. Future application of vibrational analysis to data from mutated proteins may provide insight into how specific residues in the enzyme active site are affecting the contribution of coupled motion and tunneling to reaction coordinate structure.

**Acknowledgment.** Dr. W. Saunders is thanked for providing the program BEBOVIB IV and Dr. P. Huskey is acknowledged for valuable advice, especially in the early phases of these experiments. Dr. Amnon Kohen is thanked for his critical reading of this manuscript and many useful comments. This work was supported by funding from the National Science Foundation (MCB 9221072),

JA9824425

(70) Bahnson, B. J.; Colby, T. D.; Chin, J. K.; Goldstein, B. M.; Klinman, J. P. *Proc. Natl. Acad. Sci.* **1997**, *94*, 12797–12802.

(71) Cook, P. F.; Blanchard, J. S.; Cleland, W. W. *Biochemistry* **1980**, *19*, 4853–4858.